JOURNAL OF APPLIED ELECTROCHEMISTRY 17 (1987) 225–242

*The chemistry and electrochemistry associated with the electroplating of group VIA transition metals**

S. H. WHITE, U. M. TWARDOCH

EIC Laboratories, Inc., 111 Downey Street, Norwood, Massachusetts 02062, USA

Received 10 April 1986; revised 5 September 1986

An overview of the requirements for the electroplating of refractory metals from molten salts is presented, followed by a discussion of recent electrochemical studies which have been carried out to delineate the solution chemistry of alkali metal halide plating baths. New results for halide baths involving chromium and molybdenum are presented and considered from the view of both solution chemistry and the electrocrystallization processes of these metals. Advantages and disadvantages of these electrolytes are discussed in the context of plating cell development and pulse modulated plating techniques.

1. Introduction

Electrodeposition of metals from molten salts has been practised successfully on an industrial scale for the winning of, for example, aluminium, magnesium, calcium, lithium and sodium [1]. Titanium, tantalum and niobium [2] have also been electrodeposited in dendritic form in large-scale operations. Electroplating, on the other hand, requires *coherent* metal formation, a severe restriction which has limited success to but a few metals which include the refractory metals, the precious metals, aluminium, etc. The focus of this paper is on the electroplating of the refractory metals, in particular those of group VIA. In the 1960s, Union Carbide announced a generalized process for electroplating refractory metals from molten fluoride electrolytes [3, 4]. Table 1 shows the operating temperature, metal ion oxidation states and reduction pathways for these processes [2, 4].

Molten alkali metal fluorides have a number of advantages as electrolytes. They are good solvents with complexing properties that enable the refractory metal cations (in a variety of oxidation states) to be stabilized in solution. High solute precursor concentrations are thereby achievable, leading to a wide range of plating conditions. The alkali fluoride solutions possess high conductivities which minimize *IR* losses at the high rates of metal deposition possible. The molten fluoride electrolyte acts as a fluxing agent to remove scale from work pieces within the electrolyte. The wide electrochemical window in these solvents provides a versatile electrolyte bath suitable for the electrodeposition in coherent form of all nine of the refractory elements at moderate cost [2]. The molten fluoride electrolyte baths possess a number of disadvantages, amongst which are the following. The operation of the electrolyte baths requires temperatures in excess of 600° C (Table 1) which limit the choice of materials for the construction of the plating cells and the substrates available as cathodes. The electrolyte can be modified by atmospheric contamination, and the plating process is sensitive to impurities such as oxide and chloride ions [5]. When lithium-containing electrolytes are used, clean up of the plated article can be a problem because of the low solubility of the salt of the fluoride and, finally, fluorides and their vapours are toxic.

Prior to, and subsequent to, the development of the Union Carbide process, alternative electrolytes have been considered for the electroplating of refractory metals. Oxyanionic melts have

* This paper was presented at a workshop on the electrodeposition of refractory metals, held at Imperial College, London, in July 1985.

0021–891X/87 $03.00 + .12

Table 1. Summary of the electrochemistry of refractory metals in molten fluoride melts

Group	*Temp. (°C)*	*Element*	*Mean valency*	*Reduction sequence*
Group IV	~700	Ti	3	$Ti^{3+} \longrightarrow Ti$
	700	Zr	4	$Zr^{4+} \longrightarrow Zr$
	700	Hf	4	$Hf^{4+} \longrightarrow Hf$
Group V	600/800	V	3	$V^{3+} \longrightarrow V$
	600	Nb	4	$Nb^{4+} \longrightarrow Nb^{+} \longrightarrow Nb$
	600/800	Ta	5	$Ta^{5+} \longrightarrow Ta^{2+} \longrightarrow Ta$
Group VI	700/1000	Cr	3(?)	$Cr^{3+} \longrightarrow Cr^{2+} \longrightarrow Cr$
	700	Mo	3.3	$Mo^{3+} \longrightarrow Mo$
	700	W	4.5	$W^{4+} \longrightarrow W$

been examined [6–8], but the ease of reducibility of the oxyanion, the strong probability for oxygen contamination through oxidation of the metal during reduction of the oxyanion, and the formation of anodic oxide films, limit the usefulness of these melts. On the other hand, early work showed that in the case of tungsten, a complex mixture of borates and tungstates could lead to the formation of coherent tungsten plates [6]. Recent results for molybdenum and tungsten [8] have suggested that molybdates and tungstates can be employed as precursors for metal formation from halide electrolytes. Liquid organic salts such as the quaternary'onium salts represent alternative solvents for plating baths. These have been considered either as a component in a mixture with aluminium halides or in the pure state [9, 10]. The aluminium chloride-based melts favour cluster compound formation [11] and are good solvents for such syntheses [12]. Experiments have failed to produce coherent metal deposits of the refractory metals from these melts [13]. The alkali and alkaline earth salts of the remaining halide ions and their mixtures perhaps offer the best alternative solvent components for the development of electroplating baths for the refractory metals (VIA). This paper discusses some recent studies in both chloride and bromide mixtures.

2. Design criteria for electroplating refractory metals

Two basic features of the system must be considered for the *a priori* design of a refractory metal plating process [2]:

(i) Electrolyte composition

(ii) The reduction pathway and metal electrocrystallization mechanisms.

In the case of electrolyte composition, the cation and anion components of the electrolyte determine the electrochemical range of stability of the electrolyte and hence the suitability of the solvent for the reduction of the refractory metal ion component. In addition, the cation and anion components play a major role in determining the solute stability and the charge requirement for the electroreduction process. The pure refractory metal compounds in high oxidation states exhibit high volatility and disproportionation chemistry [14]. In their lower oxidation states, these components are often complex compounds which involve metal–metal bonding [15] and may undergo disproportionation or polymerization. The behaviour of such species in molten electrolyte solution is not well understood and is a major task which will have to be addressed in order to improve the design of alternate plating baths. The successful use of fluoride electrolytes as plating baths probably arises from the strong complexing power of the fluoride ions, which results in the simpler solution chemistry in these electrolytes. In the case of the reduction and electrocrystallization mechanisms, it is important to know both the pathway to metal (Table 1), and the kinetics of the reduction of the metal ion to coherent metal. Previous work with liquid metals, where the electrocrystallization process is absent, shows that in molten salts at 400–500° C, the exchange current density

Table 2. Summary of the electrochemistry of tungsten

Melt	*Solute and/or mean valency*	*Temp.* (°C)	*Reduction pathway*	*No. of electrons* (n)	*Deposit form*	*Ref.*
LiF–NaF–KF	WF_6 reduction with W		W(VI) W(4.48) W(IV) W(0)	4	Coherent	[21] [22]
$AlCl_3$–NaCl	WCl_6	120–220	Electrochemical cluster formation		No metal deposit	[11]
	$KWCl_6$ K_2WCl_6 $K_3W_2Cl_9$ W_6Cl_{12}					
LiCl–KCl	WCl_6 $KWCl_6$ K_2WCl_6 $K_3W_2Cl_9$ W_6Cl_{12}	400	$W(VI) + Cl^- \longrightarrow W(V) + \frac{1}{2}Cl_2$ $W(VI) + 2Cl^- \longrightarrow W(IV) + Cl_2$ $W(VI) + W(IV) \longrightarrow 2W(V)$ $W(X) \longrightarrow W(Y)$ $W(Y) \longrightarrow Z$			[23] [24]
LiCl–KCl	WBr_5 K_2WCl_6 $K_3W_2Cl_9$	450	$W(V) \longrightarrow W(IV)$ $W(IV) \longrightarrow W(II)$ $W(II) \longrightarrow W(0)$ $2W(II) \longrightarrow W(IV) + W(0)$	1 2		[25]
Na_2WO_4–WO_3	WO_3	650–800	Unknown		W or W–Na–O	[7]
$Li_2O\,P_2O_5$/ B_2O_3 mixtures	WO_3	~900	Unknown		Coherent W deposit	[6]

for the charge transfer process is greater than 1 A cm^{-2} [16]. Recent studies have identified the importance of the metal electrocrystallization processes, that is the nucleation and growth of the new metal phase on the cathode substrate [17–20]. The details of these processes and their relationships to diffusion and reaction overvoltages remain to be determined and will be an important aspect of fundamental studies in the area of refractory metal plating in the future. The remainder of this paper concentrates upon the group VIA metals (chromium, molybdenum and tungsten) whose properties such as high melting point, hardness and corrosion resistance make them candidates for constructional materials in new technologies which operate under extreme conditions.

3. Tungsten electroplating

Table 2 summarizes briefly the features of the electrochemistry of tungsten in molten salts. As in the case in aqueous solution [14, 15] the chemistry of tungsten in molten salts is complex because of the multiplicity of oxidation states possible, and the affinity for oxygen and the sensitivity of compound stabilities in the molten solutions to the nearest neighbour electrostatic environments. In the case of fluoride electrolytes [4, 21, 22], simple reduction of gaseous tungsten hexafluoride in an alkali fluoride melt by tungsten metal leads to a plating bath which has been used on the pilot plant scale in the USA and in France. The major disadvantage with this process is the high temperature required for cell operations. Other halides have been considered [11, 23–25] and focus has centred on the use of chloride baths. Recently, a number of complex tungsten chlorides were examined in both lithium chloride–potassium chloride and caesium chloride–lithium chloride eutectic mixtures [23, 24]. On the basis of these results, it is suggested that tungsten can be obtained in coherent form from a chloride bath. The significance of this result is that alloy plating of tungsten combined with chromium and molybdenum should be

possible, since, as will be seen later, both molybdenum and chromium can also be deposited from similar halide baths at low temperatures.

4. Molybdenum electroplating

4.1. *Previous work*

It is clear from Table 3, which summarizes the electrochemistry associated with molybdenum metal plating, that considerable effort has been devoted to obtain molybdenum plates in coherent form from various halide electrolytes. Early work showed that aluminium chloride-containing melts were unsuitable for the preparation of molybdenum metal [27, 35, 36]. Senderoff and Brenner [27] demonstrated that molybdenum could be plated from a lithium chloride–potassium chloride mixture containing potassium hexachloromolybdate at temperatures between 600 and 800° C. Senderoff and Mellors also reported that molybdenum could be plated from molten fluoride electrolytes by preparing the bath from molybdenum hexafluoride and reducing the molybdenum species in solution with molybdenum metal to a mixed three/four oxidation state [4, 22]. Although the latter baths gave good deposits, the stability of that electrolyte was rather unsatisfactory [22]. Senderoff and Mellors [26] reported on the basic electrochemistry associated with the lithium chloride–potassium chloride baths used by Senderoff and Brenner. They proposed that there were two molybdenum (III) species in the electrolyte bath in equilibrium:

$$(Mo_2Cl_9)^{-3} + 3Cl^- \rightleftharpoons 2(MoCl_6)^{-3} \quad (1)$$

and that this was coupled to the disproportionation reaction:

$$5(MoCl_6)^{-3} \longrightarrow 2Mo + 3MoCl_5 + 15Cl^- \quad (2)$$

The evidence for this deduction was based upon the increased melt stability as the concentration of the solute was raised. Their chronopotentiometric results were consistent with Sand's equation and provided no evidence to support the coupling of Equation 1 with the electrode reaction at any of the temperatures examined (600–800° C). Subsequent studies by other workers have provided somewhat tentative support for this CE-type mechanism [30, 33, compare 31].

4.2. *Present studies*

Recently, studies [38] have been carried out with the lithium chloride–potassium chloride and the lithium chloride–caesium chloride electrolytes which were chosen to contrast the stabilities of the $[Mo_2Cl_9]^{-3}$ ions. The experiments have provided a number of pertinent results. It has been found that stable solutions are obtained after some 24–48 h at a temperature of 500° C; that there is a strong temperature dependence of the electrochemical responses especially in the voltammetric results; that the electrochemical response is a function of the electrochemical observation time; and under specific conditions of temperature and scan rate or current density evidence was obtained for molybdenum metal deposition.

During the initial period after melting of the electrolyte, yellow crystals were seen to condense in an air-cooled tower mounted on the top of the electrolytic cell. At the same time and in separate experiments, cyclic voltammetric measurements showed that changes in the details of the electrochemical response were occurring (see Fig. 1). The peak at 0.25 V was identified as being due to the reduction of MoO_2Cl_2 which had been studied previously by Popov and Laitinen [34]. On the basis of their value of the diffusion coefficient for this species, it was estimated that the potassium hexachloromolybdate which was used in the present experiments contains some 0.5–1.0% MoO_3. After the evolution of yellow MoO_2Cl_2, the solutions were stable and the electrolyte bath was used for electroplating for an excess of 30 days. The earlier stability problems associated with the use of molybdenum (III) chloride solutions could have arisen from either oxyanion impurities in potassium hexachloromolybdate or in the solvent itself [26, 27].

The details of the electrolyte solution chemistry have remained speculative in spite of a number of efforts to obtain quantitative results [30, 33, 38]. The present results provide further support for the suggestion that Equation 1 is important for the description of these solutions and the

Table 3. Summary of the electrochemistry of molybdenum

Melt	*Solute and/or mean valency*	*Temp.* (°C)	*Reduction pathway*	*No. of electrons* (n)	*Deposit form*	*Ref.*
LiF–NaF–KF	MoF_6 + Mo (3.3)	800	Mo(III) ⟶ Mo(0)	3	Coherent	[22]
LiCl–KCl	K_3MoCl_6	500–800	Mo(III) ⟶ Mo(0)	3	Coherent	[26, 27]
		500–800	Mo_2(III) ⟶ 2Mo(III)			
			Mo(III) ⟶ Mo(0)	3		
			Mo(III) 2/5Mo(0) + 3/5Mo(V)			
LiCl–KCl	K_3MoCl_6	450	Mo/Mo^{3+}	3		[28, 29]
LiBr–KBr	K_3MoBr_6					[30]
LiCl–KCl	K_3MoCl_6				Coherent	[31]
LiCl–CsCl	(CO_2)	670–800				[32]
NaCl–KCl	Mo anodic	760	Mo_2(III) ⟶ 2Mo(III)			
(20 80 mol %)	dissolution		Mo(III) ⟶ Mo(0)	3		[33]
	(Mo(III)					
LiCl–KCl	MoO_3	450	Mo(VI) ⟶ Mo(IV)	2	No metal deposit	[34]
	$MoO_2Cl_3^2$					
	Mo_2O_7					
	MoO_2Cl_2					
NaCl–$AlCl_3$	$MoCl_5$	175	Mo(V) ⟶ Mo(III)	1	No metal	[36]
			Mo(IV) ⟶ Mo(III)	1	deposit	
			Mo(III) ⟶ Mo(III)			
			or			
			Mo(V) ⟶ Mo(III)			[37]
			Mo(III) ⟶ Mo(II)	1		
			Mo(II) ⟶ Mo(0)			
$AlCl_3$–BPC	$MoCl_5$	RT	Mo_2(V) ⟶ 2Mo(V)	1	No metal	[9]
(acidic)			Mo(V) ⟶ Mo(IV)			
$AlCl_3$–IC	$MoCl_5$		Mo(V) + solvent ⟶ Mo(IV)	1	Spectrn.	[10]
	K_3MoCl_6		Mo(IV) ⟶ Mo(III)		electrochem.	
LiCl–KCl and other chloride mixture	K_3MoCl_6	350–530	2Mo(III) ⟶ Mo_2(III)		Coherent	[38]
			Mo_2(III) ⟶ Mo(0)			
			and			
			Mo(III) ⟶ Mo(0)			

BPC = butylpyridinium chloride
IC = 1-methyl-3-ethyl imidazolium chloride

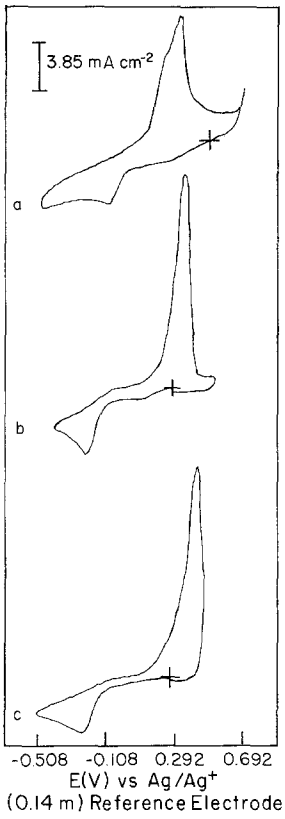

Fig. 1. Time dependence of the voltammetric responses for a solution of K_3MoCl_6 (0.013 molal) in LiCl–CsCl at 450° C: (a) 1.5 h after the mixture was molten; (b) 18 h after the mixture was molten; (c) 62 h after the mixture was molten.

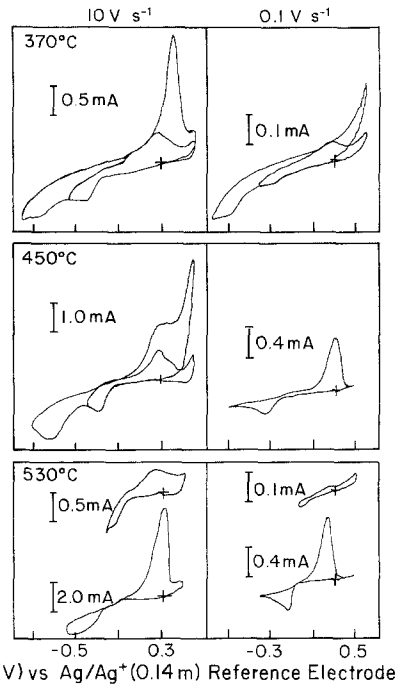

Fig. 2. Influence of temperature and scan rate on the cyclic voltammetric responses at a gold working electrode in a solution of K_3MoCl_6 (0.013 molal) in LiCl–CsCl.

design of plating baths. Fig. 2 shows cyclic voltammograms obtained in the caesium chloride-containing melt at two different scan rates and three temperatures. These voltammograms are contrasted with those obtained in Fig. 3 for the lithium chloride–potassium chloride melt at 450 and 500° C. These results show that the solution chemistry depends strongly on the melt cations as well as the operating temperature. The dependence of the voltammetric responses on the scan rate also suggests that there are processes taking place coupled to the electrode reaction which are frequency-dependent. The observation of two cathodic peaks and only one reverse anodic peak in the caesium-containing melt is consistent with the presence of two different forms of molybdenum in the same oxidation state (see also [33]). Electrodeposition experiments (loc. cit.) showed that molybdenum metal was formed and that three electrons are involved in the reduction process. Voltammograms at high temperature (530° C) and low scan rate $< 100\,mV\,s^{-1}$ in the caesium chloride-containing melt are characteristic of the formation of an insoluble metal product [39].

Chronopotentiometric results provide further evidence that the solution equilibrium (Equation 1) is coupled to the electroreduction stage. Table 4 shows the behaviour of $j\tau^{\frac{1}{2}}$ as a function of j for both transition times, and Fig. 4 shows the expected behaviour of $E_{\tau/4}$ as a function of current density.

$$E_{\tau/4} = E^0 + B \ln (K/1 + K) + B \ln (C - zj) \qquad (3)$$

where K is the equilibrium constant for Equation 1, B is a function of RT/F, C is the concentration of $[MoCl_6]^{-3}$, z is a constant and j is the current density. The quantitative analysis of the processes is complicated by the coupling of the preceding reaction step to one in which metal formations occur with a significant electrocrystallization overpotential.

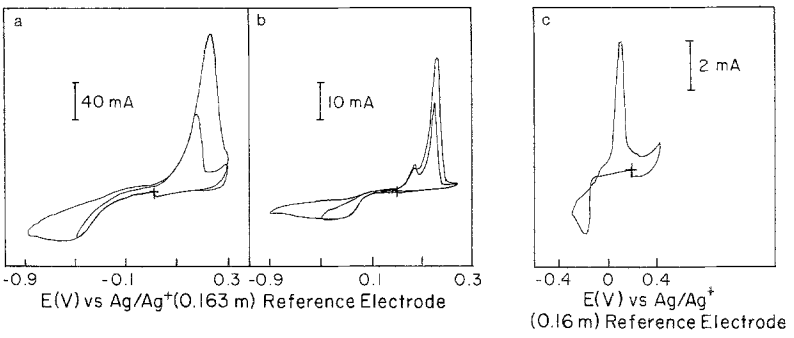

Fig. 3. Cyclic voltammograms acquired on gold electrodes in LiCl–KCl containing K_3MoCl_6. (a) At 450° C; area = 0.43 cm^2 v = 10 $V s^{-1}$; c = 19.7 × 10^{-3} mol kg^{-1}. (b) At 450° C; area = 0.43 cm^2; v = 0.1 $V s^{-1}$; c = 19.7 × 10^{-3} mol kg^{-1}. (c) At 550° C; area = 0.40 cm^2; v = 0.05 $V s^{-1}$; c = 5.06 × 10^{-3} mol kg^{-1}.

Evidence for the electrocrystallization of molybdenum metal during the deposition process has recently been obtained in studies both in the lithium chloride–potassium chloride and the lithium chloride–caesium chloride melts. Details of the formation of the new phase which involves an overpotential have been provided by cyclic voltammetric, chronopotentiometric and potential step experiments. Fig. 5 shows an example of chronopotentiogram with a nucleation overpotential in the initial region. Fig. 6 shows a series of current–time curves obtained for each solvent when increasingly negative potential steps were applied to the cathode. The current maxima and the time at the current maxima of these transients were analysed in terms of the spherical diffusion model of Gunawardena *et al.* [40]. Fig. 7 shows plots of $i^2_{max} t_{max}$ as a function of η for the two solvents. The large (tenfold) change in $i^2_{max} t_{max}$ observed for the LiCl–KCl melt is interpreted to be due to the effects of the coupled chemical reaction. A value of K' = 0.012 mol l^{-1} is calculated for Equation 1. This behaviour is in contrast to the small changes in the function $i^2_{max} t_{max}$ in the caesium chloride-containing melt. This latter result is consistent with a transition from progressive nucleation at low overvoltage to one involving instantaneous nucleation at the higher overvoltages suggesting that although the equilibrium may favour the dimer, the chemical rate constants are such that conversion to the electroactive monomer occurs at the frequencies utilized in these experiments.

The successful plating of molybdenum from both the lithium chloride–potassium chloride and lithium chloride–caesium chloride melts has been achieved. Table 5 illustrates some typical results. Fig. 8 shows a longitudinal section of molybdenum plated on a nickel substrate. The good throwing power of this process is well illustrated in this figure. An electron image obtained by the Robinson back scattering technique is shown in Fig. 9, together with an analysis of the interface by energy dispersive X-ray spectroscopy which showed that at this point the composition of the metal is close to 100% molybdenum.

In summary, evidence has been presented

Table 4. Typical chronopotentiometric data on a gold electrode for the reduction processes in a solution of potassium hexachloromolybdate (1.3 × 10^{-2} mol kg^{-1}) in caesium chloride–lithium chloride molten mixture at 530° C

j × 10^2 ($A cm^{-2}$)	τ^c_1 (s)	$E^1_{\tau/4}$ (v)	$j\tau_1^{\frac{1}{2}}$ × 10^3 $A s^{\frac{1}{2}} cm^{-2}$	τ^c_2 (s)	$E^2_{\tau/4}$ (v)	$j\tau_2^{\frac{1}{2}}$ × 10^3 ($A s^{\frac{1}{2}} cm^{-2}$)	$(\tau_1 + \tau_2)^{\frac{1}{2}} j$ × 10^3 ($A s^{\frac{1}{2}} cm^{-2}$)
5.357	0.00113	−0.180	1.786	0.0285	−0.425	9.036	9.221
3.571	0.00325	−0.155	2.035	0.064	−0.338	9.018	9.261
2.679	0.0045	−0.135	1.797	0.094	−0.287	8.196	8.408
1.428	0.0138	−0.075	2.089	0.288	−0.170	7.661	7.845
1.258	0.034	−0.070	2.321	0.360	−0.160	7.500	7.896
0.893	0.028	−0.060	1.482	0.663	−0.140	7.268	7.423
0.714	0.038	−0.050	1.393	1.050	−0.130	7.321	7.448
0.536	0.06	−0.045	1.313	1.86		7.303	7.427

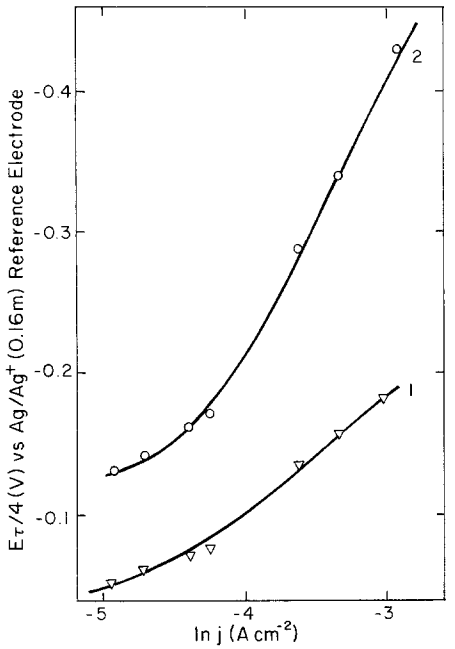

Fig. 4. The relationship between $E_{\tau/4}$ and applied current density for each transition time (1 for τ_1| and |2 for τ_2) acquired at a gold electrode in a solution of K_3MoCl_6 (13×10^{-3} M) in LiCl–CsCl at 530° C.

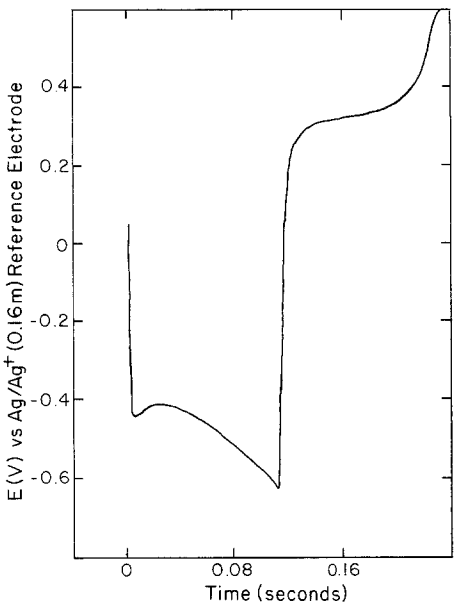

Fig. 5. Chronopotentiogram acquired at a gold electrode in LiCl–KCl containing 0.0197 molal K_3MoCl_6 at 450° C, current pulses $\pm 70\,mA\,cm^{-2}$.

which supports the interpretation of the solution chemistry in terms of Equation 1. The equilibrium constant reported at 450° C enables actual solution species concentrations to be evaluated. The results show the influence of both temperature and solvent cation composition on Equation 1 which is coupled to the electrochemical step and so plays a role in the metal deposition process. Thus, the quantitative prediction of the optimum conditions for plating, and in particular pulse plating, is more difficult. It will be necessary to quantify the equilibrium with respect to both melt cations and anions as well as the temperature in order to enable low temperature

Table 5. Pulse plating of molybdenum from alkali metal chloride melt at 530° C

Electrode No.	*Applied current (A)*	t_{off}/t_{on}	*Electrolysis time (s)*	*% current efficiency*	*Pulse or d.c.*	*Comments*
E-2-1-Ni	0.020	–	8400	41	d.c.	T = 500° C, adherent flakes
E-2-3-Ni	0.300	90	79550	85	P	Good clean, grey deposit
E-2-31-Ni	0.300	90	81402	89	P	Deposit flaked off substrate
E-2-32-SS	0.300	90	82740	94	P	Grey deposit, some dendrites
E-2-33-SS	0.150	90	89590	81	P	Grey deposit
E-2-34-SS	0.500	150	157190	91	P	Grey deposit, adherent flakes and some dendrites
E 2-20T-Ni	0.300	90	82736	50	P	Bright grey, smooth deposit after washing
E-2-27T-Ni	0.300	90	169456	77	P	Grey deposit, some flakes at three-phase boundary
E-2-37-Mo	0.300	90	230520	90	P	Bright deposit
E-2-36F-Ni	0.900	90	53543	88	P	Bright deposit

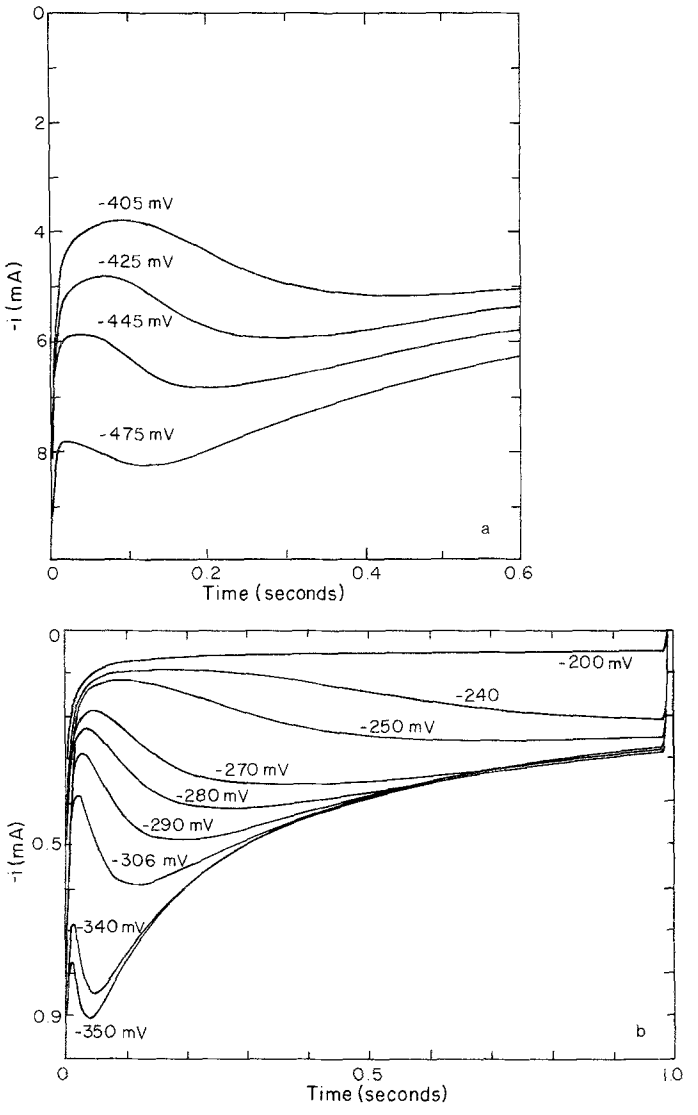

Fig. 6. Current–time transients acquired at gold electrodes in different solvents for the reduction of Mo(III) at different overpotentials versus Mo^{3+}/Mo. (a) Gold area 0.43 cm^2; 450° C; LiCl–KCl. (b) Gold area 0.056 cm^2; 530° C; LiCl–CsCl.

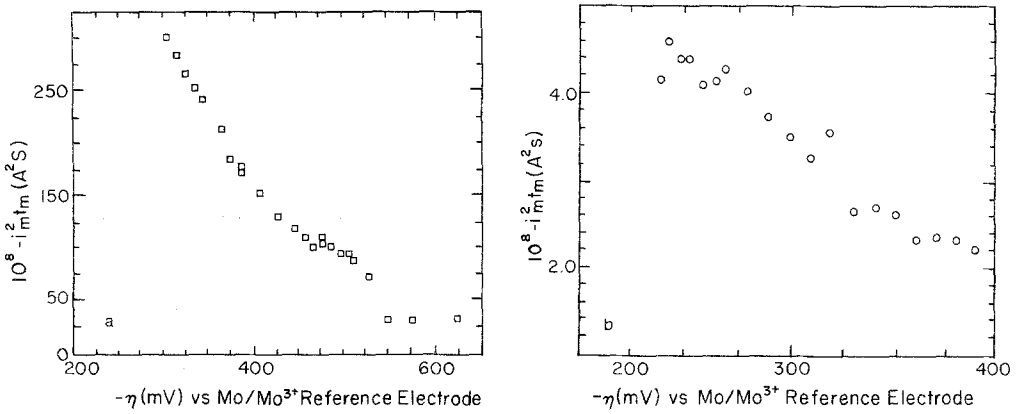

Fig. 7. Plots of $i_m^2 t_m$ versus applied overpotential for molybdenum deposition on a gold substrate in: (a) LiCl–KCl at 450° C; (b) LiCl–CsCl at 530° C. Currents in (a) normalized to electrode area in (b).

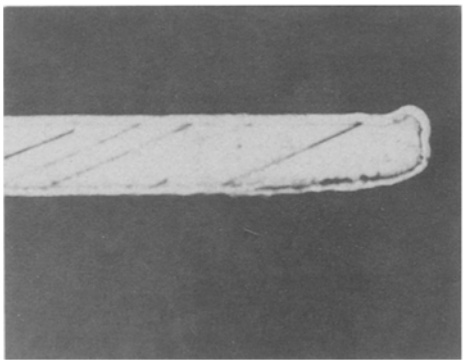

Fig. 8. Longitudinal section of nickel electrode plated with molybdenum at ×25. Note the good throwing power as exemplified by the plate following the contour of the end of the electrode.

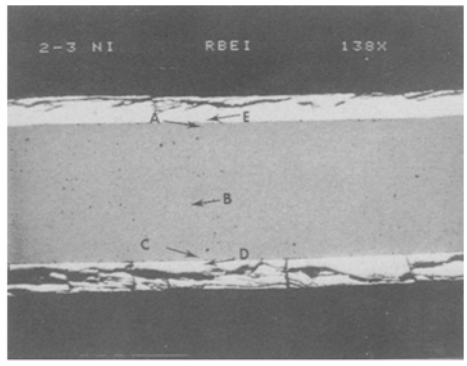

Fig. 9. Robinson back scattered electron image of the cross-section of a molybdenum-plated nickel electrode. Points A to E were analysed for elemental content, and the following results were obtained. Nickel content (wt %): A, 100; B, 100; C, 100; D, 3; E, 3. Molybdenum content (wt %): A–C, zero; D, 97; E, 97. ×72.

processes to be optimized. Such studies should enable the design of electroplating baths and conditions for molybdenum deposition to be developed, and work is continuing in this direction.

5. Chromium electroplating

5.1. *Previous work*

Table 6 summarizes studies made in recent years on the electrochemistry of chromium in fluorides, chlorides, bromides and aluminium chloride-containing melts. The major focus of attention has been on the use of chloride melts. However, it was shown that fluoride melts operating at temperatures in excess of 800° C enable coherent deposits of chromium [4, 41] to be obtained. The solution chemistry of these melts has been difficult to resolve in spite of efforts by both Mellors and Senderoff [41] and Yoko and Bailey [46], and it is unclear at this time whether the electroactive species present in the solution of the molten fluoride is a chromium(IV) or a chromium(III) species. In constrast to the fluoride electrolytes, chloride and bromide melts containing chromium(III) or (II) ions have been investigated and shown to possess a simpler solution chemistry. Chromium metal has been plated from both of these electrolytes (17, 18, 45] and it is pertinent to explore the reasons for the apparent ease by which these melts yield coherent metal.

The solution chemistry of chromium(II) and chromium(III) halides is straightforward. Spectroscopic studies suggest that chromium(III) ions are present in alkali metal chloride (and bromide) melts as octahedral complexes $[CrX_6]^{-3}$. Spectroscopic studies of chromium(II) ions in the same melts show a band at 9800 cm^{-1}, but the nature of the configuration responsible for this spectrum has not been identified [55]. However, it has been suggested that on the basis of other first-row transition metal divalent ions the chromium(II) halocomplex present in the melts is a distorted tetrahedral species [51]. Chromium(II) ions are readily reduced by a two-electron transfer to metal in both alkali chloride [17, 18] and bromide [45] solutions. On the other hand, oxidation of chromium(II) takes place in these melts via a one-electron process to the chromium(III) species. This latter oxidation process allows the measurement of the diffusion coefficients of chromium(II) ions without the complications associated with electrocrystallization phenomena which normally arise in the reduction process to metal. Fig. 10 shows the reduction of chromium(II) ions to chromium metal in a chloride melt at 450° C and in a bromide melt at 273° C. The magnitude of the diffusion coefficient obtained in the bromide melt at 273° C ($D = 0.2 \times 10^{-5}$ $cm^2 s^{-1}$) suggests that this melt is suitable for the electrodeposition of chromium metal.

Consequently, it is concluded that chromium(II) ions in molten alkali chloride or bro-

Table 6. Summary of the electrochemistry of chromium

Melt	*Solute and/or mean valency*	*Temp. (°C)*	*Reduction pathway*	*No. of electrons (n)*	*Deposit form*	*Ref.*
LiF–KF–NaF	CrF_4	900	Cr(IV) $\longrightarrow$ Cr(0)	4	Coherent	[41]
LiCl–KCl	Cr anodization to Cr(II) and oxidation to Cr(III) and $CrCl_2$ addn.	450–500	Cr(III) $\longrightarrow$ Cr(II) Cr(II) $\longrightarrow$ Cr(0) (irr.)	1 2	Coherent	[18, 42]
LiCl–KCl NaBr, KBr	$CrCl_2$	550–750	Cr(II) $\longrightarrow$ Cr(0)		Dendrite	[43]
LiCl–KCl	Cr anodization	450	Cr(III) $\longrightarrow$ Cr(II)			[17]
LiBr–KBr–CsBr	Cr(II)	270–450	Cr(II) $\longrightarrow$ Cr(0) rev.	2	Coherent	[45]
LiCl–KCl	$CrCl_3$	500	Cr(III) $\longrightarrow$ Cr(II) Cr(II) + $2Cl^-$ $\longrightarrow$ $CrCl_2$ (insoluble) and Cr(II) $\longrightarrow$ Cr(0)	1 2		[44]
LiF–NaF–KF	CrF_3	550–1000	Cr(III) $\longrightarrow$ Cr(II) Cr(II) $\longrightarrow$ Z Z $\longrightarrow$ $(x/2)$Cr(0) Z $\longrightarrow$ Cr(III)	1 (x)	Coherent above 900° C	[46]
NaCl–$AlCl_3$ 1 : 1 1 : 2	$CrCl_3$	175	Cr(III) $\longrightarrow$ Cr(II) Cr(III) $\longrightarrow$ Cr(II) (ads) Cr(II) $\longrightarrow$ Cr(0) Cr(I)ads $\longrightarrow$ Cr(0)	1 1 2	No deposit	[47]
LiCl–KCl	$CrCl_3$	450	Cr(III) $\longrightarrow$ Cr(II) Cr(III) $\longrightarrow$ Cr(0)	1 2		[48]
NaCl–KCl		700	Cr(III) + $2e$ $\longrightarrow$ Cr(II) Cr(III) + $2e$ $\longrightarrow$ Cr(0) irr	1 2		[49]
LiCl–KCl	$CrCl_3$	450	Cr(III) $\longrightarrow$ Cr(II) $[CrCl_5OH]^{3-}$ $\longrightarrow$ $[CrCl_5OH]^{4-}$	1 1		[50, 51]
NaCl	$CrCl_2$	815–1015	Cr(II) $\longrightarrow$ Cr(0) rev.	2		[52]
NaF–CaF_2	CrF_2	1050–1100	Cr(II) $\longrightarrow$ Cr(0)		Chromium	[53]
LiF–NaF–KF	CrF_2 CrF_3 TaF_5	800–900			Coherent Cr and Cr/Ta alloy	[54]

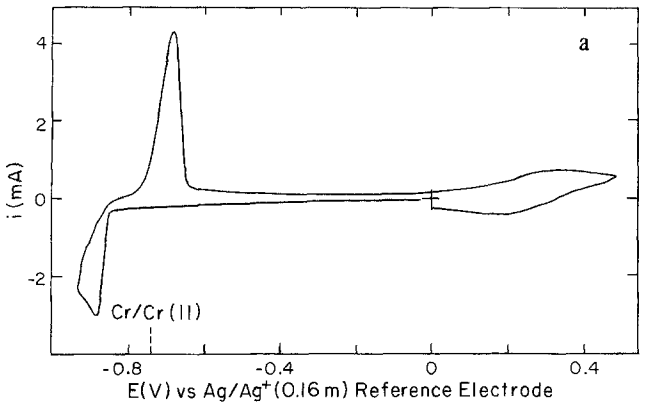

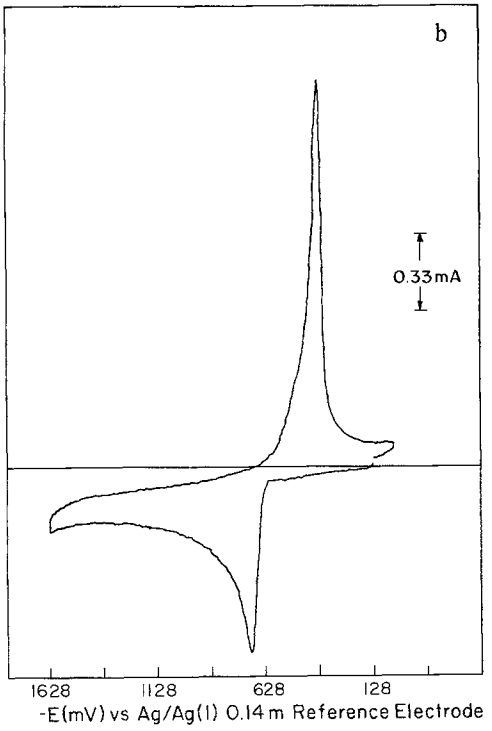

Fig. 10. Voltammograms illustrating the redox behaviour of Cr(II) ions in (a) chloride and (b) bromide melts. Scan rate = $0.100\,V\,s^{-1}$.

mide solutions are relatively easy to use for metal deposition because chemical processes in these solutions involve simple complex ions whose transitions are rapid and transport-controlled in contrast to molybdenum and tungsten (*vide supra*). However, a number of complications have been identified, particularly as more detailed studies are made, which still require complete resolution. Three areas will be discussed which are significant in the development of a high temperature (HT) chromium plating process. Two are concerned with the intrinsic properties of the electrode–electrolyte system and the third results from the interaction of the system with the atmosphere. These are therefore: (i) adsorption phenomena, (ii) chemistry coupled to the electrode process and (iii) sensitivity of the electrolyte to moisture and oxygen.

Reactant adsorption has been reported to occur during the reduction of chromium(II) ions on a chromium substrate [42]. Present studies on

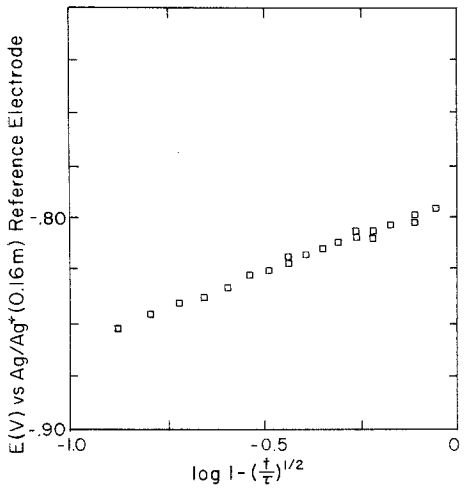

Fig. 11. Potential–time analysis of galvanostatic transient for chromium deposition on chromium-coated copper. The slope gives $n = 1.999$ and from the intercept, $E_{\tau/4}$ is calculated to be -0.811 mV versus reference. $E_{\tau/4} = -0.763$ V based on E^0 and concentration.

foreign substrates employing both cyclic voltammetry and chronopotentiometry have not detected the influence of adsorption, although this could be because of the masking effect of the electrocrystallization phenomena (loc. cit.). Analysis of potential–time data for the reduction of chromium(II) ions onto a chromium-coated copper electrode [45] showed the expected behaviour for a unit activity surface (Fig. 11). It can be concluded that under these conditions, reactant adsorption does not play a role in the reduction of chromium(II) ions.

Reactions which follow the electrochemical step have been identified when chromium(III) ions are reduced to chromium(II) ions. Levy and Reinhardt [44] and Laitinen and co-workers [51] reported that the peak current for the reoxidation process divided by the peak current for the reduction process was less than unity at low scan rates. Levy and Reinhardt interpreted their results as due to the insolubility of chromium(II) chloride [44]. It is generally recognized that chromium(II) chloride is soluble in the lithium chloride–potasssium chloride solvent [51] and therefore an alternative mechanism is necessary. It has been suggested that an explanation is to be found in the geometric changes which are possible when chromium(III) ions in the octahedral coordination are reduced to chromium(II) ions which require some modified tetrahedral coordination. Recent results for the oxidation of chromium(II) ions to chromium(III) ions on a vitreous carbon electrode show no evidence for follow-up chemistry which might be expected on the basis of a model requiring a change in the coordination geometry [45]. It is possible that the differences between the work of Laitinen and co-workers and the present study is to be found in the lability associated with different chromium complexes [14].

The sensitivity of chromium(II) and chromium(III) ions to moisture and oxygen is of some significance to the design of a chromium plating process. Laitinen *et al.* [51] showed that when melts containing chromium(III) were exposed to moist hydrogen chloride, the formation of hydroxychloro complexes took place:

$$(CrCl_6)^{-3} + H_2O \longrightarrow (CrCl_5OH)^{-3} + HCl \quad (4)$$

The subsequent coupling of the hydroxypentachloro complex ions to form an oxygen bridge compound appears to take place in an irreversible manner and ultimately leads to an insoluble product:

$$2(CrCl_5OH)^{-3} \longrightarrow (Cl_5CrOCrCl_5)^{-6} + H_2O \quad (5)$$

Although these reactions are not necessarily a direct problem with chromium(II) baths, it is known that chromium(II) species are sensitive to oxygen so that reaction will lead to the formation of chromic chloride as well as Cr_2O_3:

$$12CrCl_2 + 3O_2 \longrightarrow 2Cr_2O_3 + 8CrCl_3 \quad (6)$$

Thus, the presence of small amounts of chromic chloride in a bath of contact with moist atmospheres will ensure the formation of these oxygen bridge species. It is likely that oxide occlusions experienced with deposited metal from chromium(II) plating baths may arise because of parallel reduction of the hydroxy species formed by the mechanisms indicated above.

Recently, studies have shown that the reduction of chromium(II) to chromium metal requires a considerable overpotential at foreign cathodes.

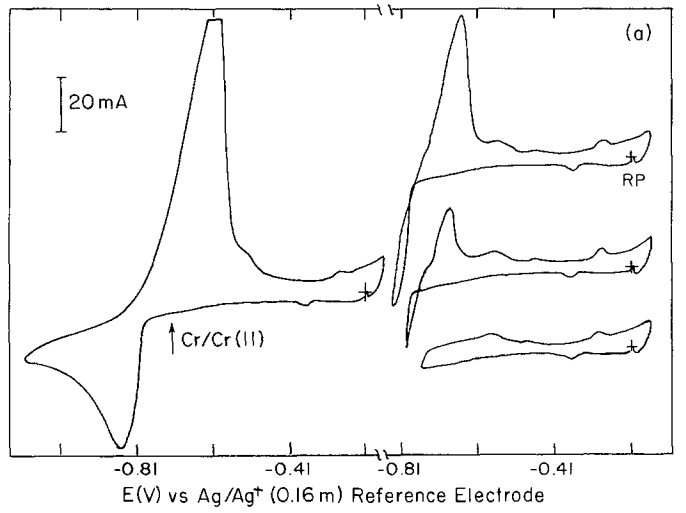

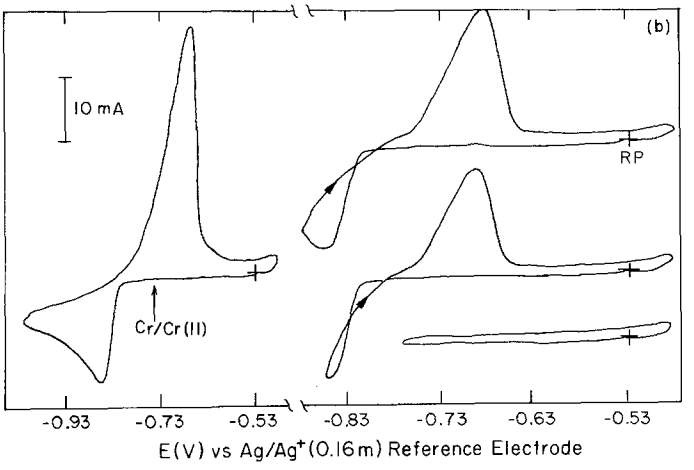

Fig. 12. Cyclic voltammograms illustrating overpotential deposition of chromium and the influence of switching potential on 'nucleation cross-over effect' in the return current sweep for (a) nickel and (b) copper substrates in LiCl–KCl containing 13 mM Cr(II) at 450° C.

Evidence for these overpotentials has been obtained on copper, nickel, gold, platinum and tungsten. Fig. 12a shows the cyclic voltammetric response on a nickel electrode when the switching potential is made more negative. The cross-over of the current on the reverse sweep corresponds to a process associated with nucleation, and similar results for copper are shown in Fig. 12b. Substantial overpotentials are observed in the initial portion of chronopotentiograms obtained on copper electrodes as shown in Fig. 13. A series of current–time curves at different applied overpotentials for the reduction

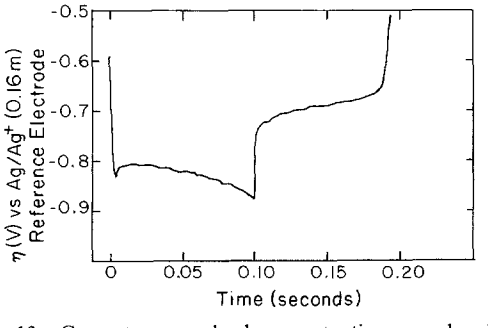

Fig. 13. Current reversal chronopotentiogram showing nucleation overvoltage at a copper electrode for Cr(II) reduction in molten LiCl–KCl at 450° C. Current pulse = 100 mA cm^{-2}.

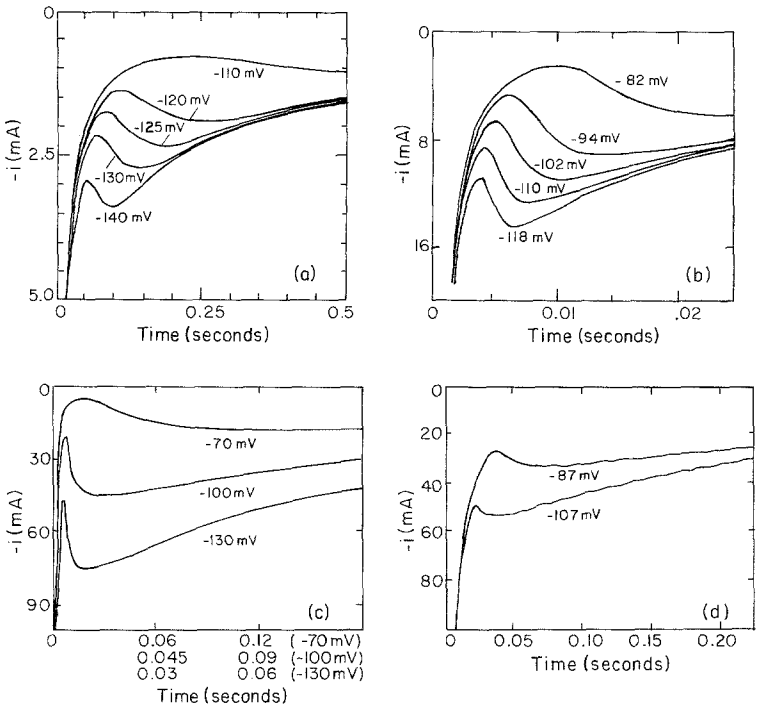

Fig. 14. Current–time curves obtained for the deposition of chromium on several substrates at different overpotentials. (a) Gold area = 0.40 cm^2; $C_{Cr(II)} = 8 \times 10^{-3}$ molal. (b) Platinum area 0.14 cm^2; $C_{CrII} = 8 \times 10^{-3}$ molal. (c) Copper area = 0.5 cm^2; $C_{Cr(II)} = 14 \times 10^{-3}$ molal. (d) Nickel area = 0.6 cm^2; $C_{Cr(II)} = 14 \times 10^{-3}$ molal.

of chromium(II) on different substrates in lithium chloride–potassium chloride at 450° are illustrated in Fig. 14. In all cases, analysis of the region prior to the maximum in the current was attempted but resolution between the time dependence of the current ($t^{\frac{3}{2}}$ and/or $t^{\frac{1}{2}}$) is poor. The behaviour of the current maxima and time at the current maxima in the current–time curves at different overpotentials was therefore employed.

Typical plots of i_m versus $t_m^{-\frac{1}{2}}$ are presented in Fig. 15. The positive deviation in the currents at shorter times arise from contributions from the nucleation process. The slope of the plots in Fig. 15 is given by:

$$nFACD^{\frac{1}{2}}Q^{\frac{1}{2}}$$

where Q is 0.26 for progressive nucleation and 0.16 for instantaneous nucleation [40]. Anodic current–time data were obtained for the same gold and platinum electrodes in these solutions, and the value of $ACD^{\frac{1}{2}}$ deduced from the i_A versus $t^{-\frac{1}{2}}$ plots for the reaction

$$Cr^{2+} \longrightarrow Cr^{3+} + e \qquad (7)$$

With the appropriate value of $n = 2$, Q was

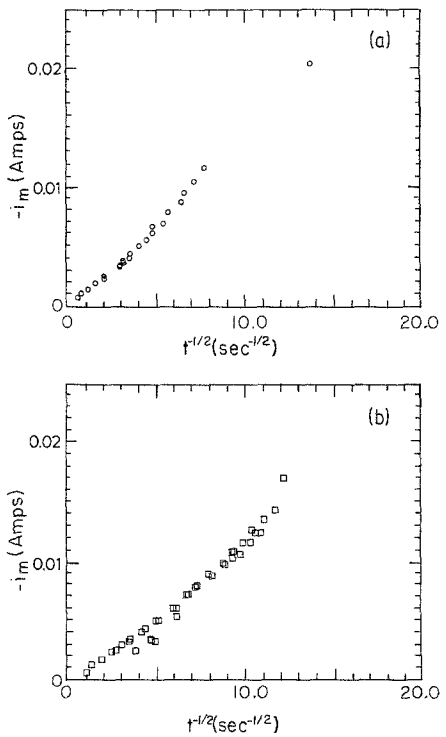

Fig. 15. Plots of i_{max} versus $t_{max}^{-\frac{1}{2}}$ for chromium deposition on (a) gold, (b) platinum substrates in LiCl–KCl at 450° C.

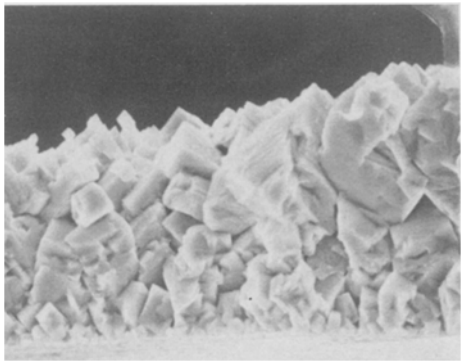

Fig. 16. Cross-section of deposit of chromium on stainless steel at 340° C from ternary alkali bromide melt. × 1050.

found to be close to 0.16 for both electrodes, showing that instantaneous nucleation had been reached. The arrest in the nucleation process had arisen from complete overlap of the diffusion zones around the nuclei. Similar results were obtained for nickel. Since t_m is directly proportional to the applied overpotential, the number and size of the crystallites can be controlled by the characteristics of the modulated pulse plating wave form. The use of a conditioning controlled potential prior to controlled potential electrolysis as well as pulsed current electrolysis has recently been reported [17, 18].

One might ask how this chemistry and electrochemistry comes together in the development of a plating process for chromium. As long as the elimination of moisture and oxygen has been achieved, the solution chemistry involves only a single complex ion in solution. The electrochemical pathway to metal requires the transfer of two electrons. Under these conditions the electrocrystallization of chromium metal can be achieved. The form of the deposited metal may be controlled by the use of high overpotentials or high current densities. Under these conditions it is likely that the maximum number of active sites on the foreign substrate surface may be used and that polycrystalline growth occurs. Of course, in aqueous solution and indeed with d.c. plating in melts the high overpotential and high current densities necessary lead to severe concentration polarization [56]. In the present work, pulsed currents [45] have been used to enable high current densities to be achieved without the concomitant problems associated with concentration polarization. Experiments have demonstrated that chromium may be plated from the low melting bromide bath using pulse current. In any design of a plating procedure for low temperature deposition of chromium, the relationship between the deposit and the plating wave forms will require development. The design of the cell must allow for operation under anaerobic and anhydrous conditions. The low temperatures offer an opportunity to eliminate iron contamination which was a serious problem in related chromium refining technology [43].

Using pulsed currents with a single laboratory cell, the capability of depositing chromium from melts at around 300° C from a ternary alkali metal bromide electrolyte has been demonstrated. Fig. 16 shows a cross-section of a chromium deposit obtained on stainless steel and Fig. 17a

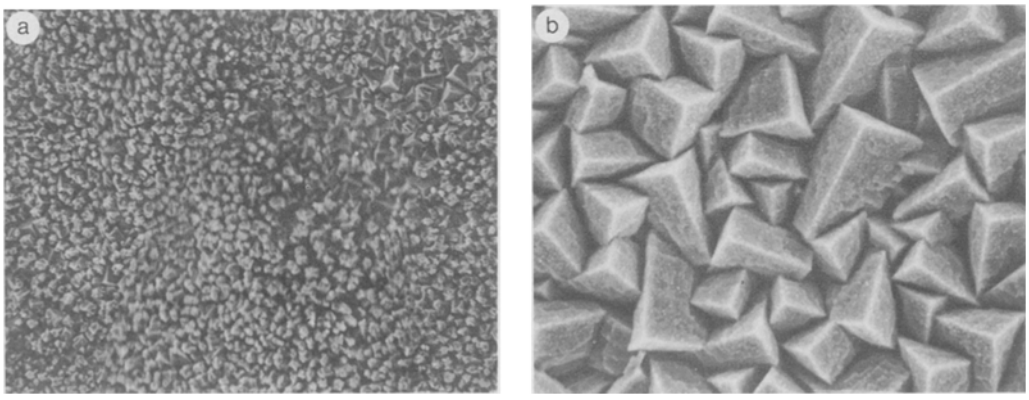

Fig. 17. SEM of chromium deposit on steel from ternary alkali bromide melt at 340° C. (a) × 280; (b) × 1120.

Table 7. Comparison of conditions for the electrodeposition of chromium from different electrolytes

Plating bath	*Aqueous*	*FLiNaK*	*LiCl–KCl*	*LiCl–KCl*	*LiBr–KBr–CsBr*
Melting pt. (°C)	< 4	454	362	362	236
Solute salt	H_2SO_4 CrO_3	CrF_3	$CrCl_2$	$CrCl_2$	$CrBr_2$
Conc. (wt %)		15	0.2–15	0.25	0.6
Operating temp. (°C)	20–60	800	450–500	450	300–340
d.c. plating j (A dm^{-2})	10–50	2–3	0.1–1	0.08	1–2
Pulse plating Potentiostatic j_{av} (A dm^{-2})	–	–	2	–	
Galvanostatic j_{av} (A dm^{-2})	–	–	–	0.23	3.2
Current efficiency	10–30	65	80	90	> 70
Plating rate (μm h^{-1})	3–70	15	28	13	20–60
Substrate composition	Cu/Ni flash	Steel	Steel	Cu, Ni	Cu, Ni, steel
Deposit adhesion	Good	Good	Poor	Good	Good/poor
Surface fluxing		Very good	---------- Unknown ----------		
Reference	[57, 58]	[54]	[18]	[17]	[45]

shows a scanning electron micrograph of the surface of a chromium deposit. The large regular cubic form of the chromium deposit is seen at high magnifications in Fig. 17b. The conditions for the electroplating of chromium from different electrolytes is compared in Table 7. A number of advantages can be seen to accrue from such procedures. The current efficiency of the process is closer to 100%. The plating rate is at least as good as for aqueous solution, and with increased solute concentration should easily surpass the aqueous plating rates. Low process temperatures, of the order of 275 to 350° C, can be used which should minimize material problems considerably. Adhesion to the substrate has been variable and coating structure is encouraging in view of the unknown relationships between the structure of the deposit and the plating parameters. These preliminary results demonstrate that a high rate, high current efficiency and low temperature molten salt plating process for chromium is possible using modulated plating methods. In conclusion, it is apparent that the development of chromium plating from alkali halides, particularly the low melting bromide electrolytes, is opportune and could lead to chromium plates with or without codeposited interstitial elements such as carbon, hydrogen or boron.

6. Experimental details

A description of the preparation and handling of materials and the electrochemical equipment and methodology is given in recent reports [59, 60].

Acknowledgements

The authors wish to thank The Army Research Office and the National Science Foundation for support of this work under Contract No. DAAG29-82-C-0015 and Grant No. DMR-8360814.

References

[1] C. L. Mantell, 'Electrochemical Engineering', McGraw Hill, 1960.

[2] D. Inman and S. H. White, *J. Appl. Electrochem.* **8** (1978) 375.

[3] S. Senderoff, *Metall. Rev.* **1** (1966) 97.

[4] G. W. Mellors and S. Senderoff, Canadian Patent 688 546 (1964).

[5] S. Senderoff in 'Modern Electroplating' (edited by F. A. Lowenheim), Wiley (1974) p. 473.

[6] B. L. Davis and C. H. R. Gentry, *Metallurgia* **53** (1956) 3.

[7] A. N. Baraboshkin, K. A. Kaliev and A. B. Aksent-'sev, *Elektrokhimiya* **14** (1978) 1836.

[8] K. H. Stern and S. T. Gadomski, in 'Proc. Fourth International Symp. on Molten Salts', The Electrochemical Society (1984) p. 611.

[9] C. L. Hussey and T. M. Laher, in Proc. Third International Symp. on Molten Salts', The Electrochemical Society (1981) p. 256.

[10] T. B. Scheffer, C. L. Hussey, K. R. Seddon, C. M. Kear and P. D. Armitage, *Inorg. Chem.* **22** (1983) 2099.

[11] D. L. Brotherton, PhD Dissertation, The University of Tennessee (1974).

[12] J. L. Meyer and R. E. McCarley, *Inorg. Chem.* **17** (1978) 1867.

[13] G. Mamantov, B. Gilbert, K. W. Fung, R. Marassi, P. Rolland, G. Torsi, K. A. Bowman, D. L. Brotherton, L. E. McCurry and G. Ting, in 'Proc. First International Symp. on Molten Salts', The Electrochemical Society (1976) p. 234.

[14] F. A. Cotton and G. Wilkinson, 'Advanced Inorganic Chemistry', Interscience (1980).

[15] F. A. Cotton and R. A. Walton, 'Multiple Bonds Between Metal Atoms', Wiley (1982).

[16] A. D. Graves, G. J. Hills and D. Inman, in 'Advances in Electrochemistry and Electrochemical Engineering', (edited by P. Delahay), Interscience (1966) p. 117.

[17] S. H. White and U. M. Twardoch, in 'Proc. Fourth International Symp. on Molten Salts', The Electrochemical Society (1984) p. 559.

[18] D. Inman, T. Vargas, S. Duan and P. G. Dudley, in 'Proc. Fourth International Symp. on Molten Salts', The Electrochemical Society (1984) p. 545.

[19] F. Lantelme and J. Chavalet, *J. Electroanal. Chem.* **121** (1981) 311.

[20] G. J. Hills, D. J. Schriffin and J. Thompson, *Electrochim. Acta* **19** (1974) 657, 671.

[21] M. Broc. G. Chauvin and H. Coriou, in 'Molten Salt Electrolysis in Metal Production', IMM London (1977) p. 69.

[22] S. Senderoff and G. W. Mellors, *J. Electrochem. Soc.* **114** (1967) 586.

[23] P. G. Dudley, D. Inman and S. H. White in 'Proc. Second International Symp. on Molten Salts', The Electrochemical Society (1981) p. 29.

[24] P. G. Dudley, MSc Thesis, London University (1980).

[25] D. Zuckerbrod and R. A. Bailey, in 'Proc. Fourth International Symp. on Molten Salts', The Electrochemical Society (1984) p. 571.

[26] S. Senderoff and B. W. Mellors, *J. Electrochem. Soc.* **114** (1967) 556.

[27] S. Senderoff and A. Brenner, *ibid.* **101** (1954) 16, 38, 31.

[28] S. Selis, *J. Electrochem. Soc.* **113** (1966) 37.

[29] *Idem, J. Phys. Chem.* **72** (1968) 1442.

[30] D. Inman and R. Spencer, 'Advances in Extractive Metallurgy and Refining', IMM (1977) paper 12.

[31] M. V. Smirnov, D. A. Ryzhik and G. N. Kazantsev, *Elektrokhimiya* **1** (1965) 59.

[32] A. N. Baraboshkin, Z. S. Martem'yanova, S. V. Plaksin and N. O. Esina, *ibid.* **13** (1977) 1807.

[33] D. Inman, R. Sethi and R. Spencer, *J. Electroanal. Chem.* **29** (1971) 137.

[34] B. N. Popov and H. A. Laitinen, *J. Electrochem. Soc.* **120** (1973) 1346.

[35] E. Marshall and L. F. Yntema, *J. Phys. Chem.* **46** (1942) 353.

[36] R. G. Verdieck and L. F. Yntema, *ibid.* **46** (1942) 344.

[37] J. Phillips and R. A. Osteryoung, *J. Electrochem. Soc.* **124** (1977) 1465.

[38] S. H. White and U. M. Twardoch, unpublished work (1984).

[39] T. Berzins and P. Delahay, *J. Amer. Chem. Soc.* **75** (1953) 555.

[40] G. Gunawardena, G. J. Hills, I. Montenegro and B. Scharifker, *J. Electroanal. Chem.* **138** (1982) 225.

[41] G. W. Mellors and S. Senderoff in 'Appl. Fund. Thermod. Metal Processing', Proc. Conf. Therm. Properties Mat., Univ. Pittsburgh (1967) p. 81.

[42] D. Inman, J. C. Legey and R. Spencer, *J. Electroanal. Chem.* **61** (1975) 289.

[43] K. P. V. Lei, J. M. Hiegel and T. A. Sullivan, *J. Less-Common Metals* **27** (1972) 353.

[44] S. C. Levy and F. W. Reinhardt, *J. Electrochem. Soc.* **122** (1975) 200.

[45] S. H. White and U. M. Twardoch, unpublished work (1985).

[46] T. Yoko and R. A. Bailey, *J. Electrochem. Soc.* **131** (1984) 2590.

[47] C. L. Hussey, L. A. King and J. K. Erbacher, *ibid.* **125** (1978) 561.

[48] I. I. Naryshkin, V. P. Yurkinskii and P. T. Stangrit, *Elektrokhimiya* **5** (1969) 1043.

[49] K. Cho and T. Kuroda, *Denki Kagaku* **39** (1971) 206.

[50] H. A. Laitinen, C. H. Liu and W. S. Ferguson, *Anal. Chem.* **30** (1958) 1266.

[51] H. A. Laitinen, Y. Yamamura and I. Uchida, *J. Electrochem. Soc.* **125** (1978) 1450.

[52] G. Stehle, J. J. Duruz and D. Landolt, *J. Appl. Electrochem.* **12** (1982) 591.

[53] P. Bowles and P. C. Newdick, *Electroplat. and Metal Finish,* January (1971).

[54] I. Ahmad, W. A. Spiak and G. J. Janz, *J. Appl. Electrochem.* **11** (1981) 291.

[55] G. P. Smith, in 'Molten Salt Chemistry' (edited by M. Blander), Interscience (1964) p. 427.

[56] K. Vetter, 'Electrochemical Kinetics', Academic Press (1967).

[57] G. Dubpernell, in 'Modern Electroplating' (edited by F. A. Lowenheim), Wiley (1974) p. 87.

[58] 'Canning Handbook on Electroplating', E. & F. N. Spon, London (1978).

[59] S. H. White and U. M. Twardoch, Final Report on Contract DMR 8360814 NSF, August 1984.

[60] *Idem,* Final Report on Contract DAAG29-82-C-0015, ARO, July 1986.